ORIGIN AND CONTROL OF INSTABILITY IN SCR/TRIAC THREE-PHASE MOTOR CONTROLLERS

Prepared by: John J. Dearth, Ph.D.
University of Alabama

1982

NASA/ASEE SUMMER FACULTY RESEARCH FELLOWSHIP PROGRAM

MARSHALL SPACE FLIGHT CENTER
THE UNIVERSITY OF ALABAMA

ORIGIN AND CONTROL OF INSTABILITY IN SCR/TRIAC THREE-PHASE MOTOR CONTROLLERS

Prepared by:	John J. Dearth, Ph.D.
Academic Rank:	Temporary Assistant Professor
University and Department:	University of Alabama Dept. of Electrical Engineering
NASA/MSFC: (Laboratory) (Division) (Branch)	 Information & Electronic Systems Guidance, Control and Instrumentation Control Electronics
MSFC Counterpart:	Frank J. Nola
Date:	August 6, 1982
Contract No:	NASA-NGT-01-002-099 (University of Alabama)

ORIGIN AND CONTROL OF INSTABILITY IN SCR/TRIAC THREE-PHASE MOTOR CONTROLLERS

by

John J. Dearth, Ph.D.
Temporary Assistant Professor of Electrical Engineering
University of Alabama
Tuscaloosa, Alabama

ABSTRACT

An SCR or triac three-phase motor controller employs three sets of antiparallel SCR's or three triacs, one connected in series with each stator winding of the motor. Normally no neutral connection is made to the motor windings. The SCR's or triacs are gated by an electronics package in response to one or more feedback signals. The controller is typically designed to perform soft starting and provide energy savings and reactive power reduction during partial loading, at idle, and during high line voltage conditions. An unusual phenomenon is known to occur in motor controllers of this type. Specifically, if the firing angle is fixed, that is if the feedback loop is opened, the system can go unstable, with low inertial loads.

The energy savings and reactive power reduction functions were initiated by the power factor controller (PFC) invented by Frank J. Nola of NASA. A three-phase PFC with soft start (MSFC size D drawing number 50M28222), developed by Mr. Nola, is examined analytically and experimentally to determine how well it controls the open loop instability, described above, and other possible modes of instability. The detailed mechanism of the open loop instability is determined and shown to impose design constraints on the closed loop system. The Nola design is shown to meet those constraints.

In addition, the Nola design has a pole near 50 Hz and another pole near 200 Hz, neither of which can be moved to a significantly higher or lower frequency without adversely affecting stability. The modes of instability which place the double bounds on these poles were not understood. These are examined and explained and the poles are shown to be located for optimum stability. The Nola design also delays the timing ramps by 6^{o} to allow the firing angle to be adequately delayed at idle without an undesirable change in mode of operation. The details of this are also examined and explained.

Although not part of the stability study, the PFC is shown to reduce the power factor as measured by utilities.

ACKNOWLEDGEMENTS

The author gratefully acknowledges the extensive orientation given by, and many helpful discussions held with his NASA counterpart, Frank J. Nola. In addition, Mr. Nola gave the author free access to several breadboards of his design and some other designs. The author also gratefully acknowledges the valuable support provided by the branch chief, Clyde Jones. The program for the computer plots was written by Ralph Kissel, who "introduced" the author to the HP9845A desk-top computer.

All NASA personnel encountered by the author during his brief tenure were helpful and friendly. It should be noted that funds for the author's stipend were provided through the Technology Utilization Office.

INTRODUCTION

A solid-state three-phase induction motor controller, of the type examined in this report, employs three sets of antiparallel SCR's or three triacs, one connected in series with each stator winding. No neutral connection is made to the motor windings. This configuration provides a practical means to rapidly control the rms voltage applied to the motor. However, an unusual phenomenon is known to occur in motor controllers of this type. Specifically, if the time of the gate trigger is fixed, that is, if no feedback is employed, the system can go unstable with low inertial loads. The instability is characterized by a growing oscillation of the current amplitude with a frequency on the order of 10 Hz. This phenomenon will be referred to as the open loop instability.

Motor controllers of the type defined above were originally considered for speed control [1], but the most common applications today are soft starting and energy savings. The solid-state switches in the controller can also economically serve additional functions, which functions in themselves would not require the speed and proportional control of a solid-state switch. Examples of such functions are over/under voltage protection, overcurrent protection, phase reversal/loss protection, and programmed or remotely controlled operation. It is significant to note that solid-state starters for large motors have been reported to be often cheaper than other reduced voltage starters and in some cases cheaper than full-voltage electromechanical starters [2].

The design of motor controllers was radically altered by the invention of the power factor controller (PFC) by Frank J. Nola of NASA. It was the PFC that introduced the energy-saving function into motor controllers. The PFC produces energy savings and reactive power reduction by reducing the rms voltage to the motor during conditions of partial load and idle. A large reduction in idle current is achieved which directly reduces the reactive power drawn at idle and reduces the iron and copper power losses.

Although other systems are briefly considered, and although the material concerning the open loop instability is applicable to all controllers of this type, the bulk of this report examines a particular controller referred to in this report as the Nola design. It is a three-phase PFC with soft start capability. A complete schematic of this circuit (MSFC size D drawing number 50M28222) is available by contacting Mr. Nola.

The feedback signal in the Nola design is the time, or angle, between the line-to-neutral voltage zero crossing and the moment of current shutoff. This angle will be referred to as the conventional power factor angle, although, due to the nonsinusoidal current waveform, this angle cannot be used in the $VI\cos\theta$ formula. The θ in this formula will be referred to as the effective power factor angle. In the Nola design, the conventional power factor angle is sensed for both polarities of all three phases. The time of current shutoff is determined by detecting the voltage across the SCR's/triacs. The DC gain of the feedback loop is carefully restricted to allow the conventional power factor angle to change under load as required to match the rms motor voltage to motor load in order to maximize energy savings. The induced EMF of the motor is also detected and used to advance the firing angle to provide quick response from idle and prevent motor stalling in response to sudden loads. Also, the gain of the feedback loop is increased at idle to enhance speed of response. Under idle conditions, the transfer function of the filter for the feedback signal flattens out below one Hz at approximately 10 dB below its DC gain. A pole occurs near 50 Hz and another pole near 200 Hz. Above idle, the AC gain is lowered somewhat. The output of the filter is compared to timing ramps, one for each phase, to set the time of gate firing. The ramps begin and end 6° past the zero crossings of the line to neutral voltages. When SCR's are used, the gates of both SCR's on a given phase are triggered for both polarities, a condition equivalent to using triacs. The gates are triggered by pulse transformers driven by a 40-kHz "gatepost" oscillator. The trigger signal persists until the end

of the timing ramp for that phase to achieve the effect of level firing. Photographs of the current waveform for idle and for various amounts of motor load are shown in Fig. 1. Note that the "double hump" shape of the current waveform is characteristic of all three-phase motor controllers of this general type.

In this report, the Nola design is examined analytically and experimentally to determine how well it controls the open loop instability and other possible modes of instability. To do this, the nature of the open loop instability is studied. Variations in time of current shutoff--that is, variations in the conventional power factor angle--alter the effective voltage applied to the motor, which, in turn, alter subsequent current shutoffs. This was suspected as the mechanism of the open loop instability [3]. However, single-phase motor controllers do not exhibit the open loop instability and three-phase motor controllers exhibit the open loop instability only over a portion of their operating range extending from a little below full on down to a point where the current humps separate. There were problems explaining these observations with the suspected mechanism, but one observation clearly supports the proposed mechanism. An open loop system, the three-phase "light-dimmer" circuit, which tends to correct for disturbances in the time of current shutoff, is known to be stable [3]. (It is significant to note that the "light-dimmer" circuit does not operate in the region where the current humps separate.)

In this report, an improved model for the suspected mechanism is developed by distinguishing between the motoring and generating portions of the cycle and by consideration of the interaction of the three line currents due to Kirchoff's current law in the absence of a neutral connection to the motor windings. The improved model is consistent with the observations listed above, with the observed effect of inertial loads, with the observed effect of connecting the neutral and with some observations made on an antiparallel SCR-diode controller.

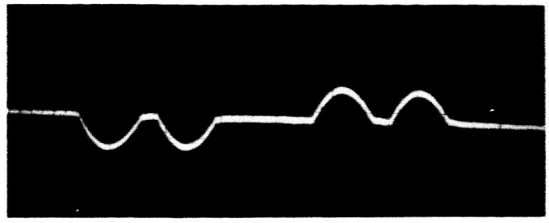

1

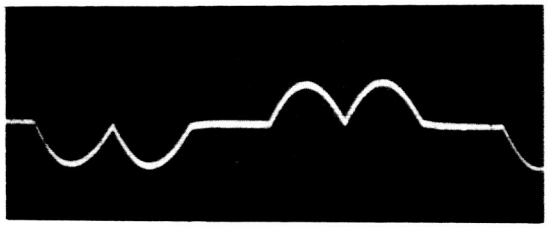

2

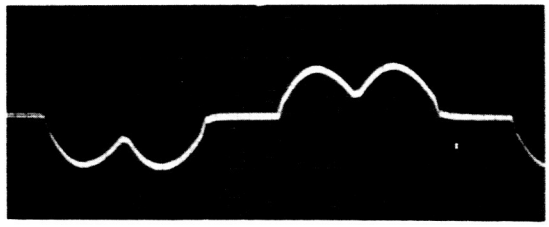

3

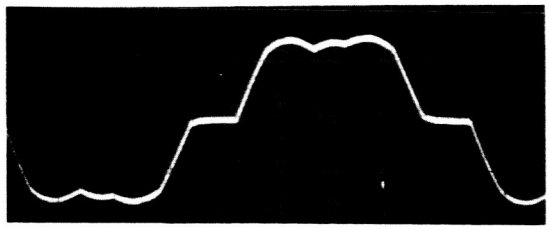

4

Fig. 1. Typical Current Waveforms For A PFC. Photograph 1 is at idle. Load increases in order 1, 2, 3, 4.

A modification of the Nola design was constructed to allow the start of the timing ramps to be referenced to the time of current shutoff and this system is stable in the open loop, as predicted by the improved model. However, this current referenced system is unstable in the closed loop--except when a very slow filter is used. The improved model is shown to impose design constraints on closed loop systems and the Nola design is shown to meet those constraints.

The second section of this report investigates the double bounds known to restrict the location of the 50-Hz and 200-Hz poles. Neither pole can be moved to a significantly higher or lower frequency without adversely affecting stability [3]. The improved model for the open loop instability is used to show that the lower bounds are required in order to control that instability. The upper bound on the 50-Hz pole and the upper bound on the 200-Hz pole are shown to be necessary to control the ripple in order to prevent matching of the ripple to the slope of the ramp, a condition which would result in very high incremental gain and erratic control.

The third section of this report determines why the 6^{o} delay of the timing ramps is required. It was known that the 6^{o} delay was necessary to allow operation in the region where the current humps do not overlap [3]. Operation in this region is essential to achieve maximum savings at idle [3, 4]. If the 6^{o} delays are removed from the circuit, it is observed that at the point where the humps are expected to separate, the second hump apparently ceases to flow and the first hump remains with a somewhat higher amplitude. This posed a paradox, because the same effect is observed in all three phases, and the second hump of any phase is the return current for the first hump of another phase. In this section, it is determined that the gate signal must persist past the zero crossing of the line-to-neutral voltage in order to retrigger the SCR/triac after the first hump has reached zero. Without the delayed turnoff of the gate signal, both humps disappear at the point in question, and the controller suffers an undesirable change to a new "single hump" mode of operation. The paradox is resolved by noting that the first hump does not actually

remain after the second hump has ceased; instead, both humps cease and a new hump forms in accordance with the new mode. It is significant to note that large delays in gate turnoff would result in premature firing, or misfiring, of the next polarity of current, since the gate signal activates both polarities with this design. However, the 6^{o} delay allows optimum savings at idle, and it is significantly less than the delay at which misfiring commences. Separate polarity triggering is discussed in the section on the optically-coupled trigger option.

The neutral point for measuring line-to-neutral voltage in the Nola design is derived by connecting equal impedances from each line to a common point. Since voltage dividers from this point are also connected to the lines after the SCR's/triacs to detect current shutoff and induced EMF, some noise is introduced into the derived neutral point. This is a consequence of the fact that opening one of the SCR's/triac switches allows the instantaneous sum of the three motor line voltages to be nonzero. Since a suitable neutral line may not be available in a typical application, the capability to operate with a derived neutral is needed. Another possible source of noise is stray coupling of the gatepost oscillation into the input of the voltage comparators which control the gate firings. The Nola design has been observed to be noise resistant and no significant effect was observed to be produced by noise. However, since these noises could be detected by careful observation with the oscilloscope, the fourth section of this report examines them and lists suggested noise reduction techniques which could be used if required by a particular application.

The Nola design was implemented with optically coupled gate trigger circuits in order to experimentally prove that the open loop instability was not a manifestation of the gatepost oscillator. In the fifth section of the report, the open loop instability is shown to occur with optically coupled trigger circuits which use no gatepost oscillator. Also, some design considerations for implementing optical coupling with the Nola circuit are discussed.

During the study covered by this report, the author was shown a copy of a paper which claimed that since the utilities measure power factor at peak demand, the PFC does not reduce the power factor penalty charged by the utilities [5]. While this might be true for a single motor, a typically plant has many motors, some of which would be idling at the time of peak demand. A calculation was made for two motors, one

at full load and one at idle to determine the effect of the PFC on the power factor of the combined load. In the sixth section of this report, the PFC is shown to reduce the power factor for the case described above.

The last section of the report discusses areas for future work.

OBJECTIVES

The basic objectives of the study reported here are to analytically and experimentally investigate the stability of the Nola design--with emphasis on the open loop instability phenomenon--and to analytically verify the choice of some empirically-determined parameters in the design. Some useful incidental information generated during the study is also reported.

OPEN LOOP INSTABILITY

The Nola design can be converted to open loop--to demonstrate the open loop instability phenomenon--by open circuiting the 15K resistor at the input to the feedback-filter amplifier. Although the induced EMF feedback is not designed to function in the operating region which is of interest here, this feedback can also be disconnected from the filter amplifier. The system is now open loop. If the grounded end of the "PFC adjust" potentiometer is, instead, connected to +15 volts, and if the soft start sequence has finished, the firing angle can be set with the PFC adjust potentiometer, as needed. To observe the instability with an unloaded motor, one gradually lowers the PFC adjust from its full negative position until the firing angle is delayed sufficiently to enter the region of instability. The unstable region is observed to begin at a hold-off angle of 5 to 20^{o} depending on the motor observed.

The other side of the unstable region is observed to be precisely limited by the point where the current humps separate as shown in the second photograph of Fig. 1. It should be mentioned that although the open loop instability will not initiate outside the region just described, the instability, once initiated within the region, can grow to where the extremes of the current swings extend beyond the region. A photograph illustrating the buildup of the instability is shown in Fig. 2. Vibration of the motor and jerky rotation of its shaft accompany the current swings. Often the power must be shut off to protect the motor. Sufficient inertia added to the motor shaft prevents the spontaneous growth of the instability, and still more inertia

quickly damps the instability in response to a torque impulse. However, loading the motor does not stop the instability, unless the load contains sufficient inertia. Although all motors exhibit the instability to some degree, some are more unstable than others.

An open loop control system with a damped oscillatory response is, of course, not unusual, but the open loop system, just described, has a negatively-damped oscillatory response--that is, it is an oscillator, and it has no apparent feedback path nor any negative resistance devices. (Although an SCR or a triac exhibits negative resistance when its forward breakover voltage is exceeded, this does not occur for this system.) Therefore an unusual mechanism must be responsible. Since the phenomenon does not occur in induction motors alone, it must be an interaction between the SCR/triac switches and the motor. Because the turn-on time is fixed, interaction can only occur via variations in the turn-off time. Consequently, the oscillations were postulated to arise in the following manner: [3]:

> If an inevitable noise disturbs the turn-off of a particular SCR or triac to a time, say, earlier than the previous turn-off, then the earlier opening of the switch means that less rms voltage is applied to the motor. Less voltage, in turn, lowers the slip and reduces the conventional power factor angle as measured at the next current zero, that is, the next turn-off is shifted earlier in time. If its shift exceeds the original disturbance, then the conditions for instability are met.

The most obvious difficulty with the proposed explanation is that it apparently also applies to single-phase motor controllers which are observed to be open loop stable [3]. In addition, the proposed explanation does not allow for the stable portions of the operating region that are observed to exist for three-phase motors, nor for the stable operation that is observed if the motor windings have a neutral connection [3]. (It is important to mention that the neutral connection is normally omitted, because it increases the stator currents required for a given torque [1].)

The model is improved, if one distinguishes between the motoring and generating portions of the cycle. The single-phase case is shown in Fig. 3. Observation of Fig. 3 reveals that at the time of current shutoff the voltage and current have opposite polarities, which implies that power is flowing from the motor to the supply line. Thus an earlier shutoff of the current returns less power to the line and supplies more net power to the motor. This is equivalent to a higher

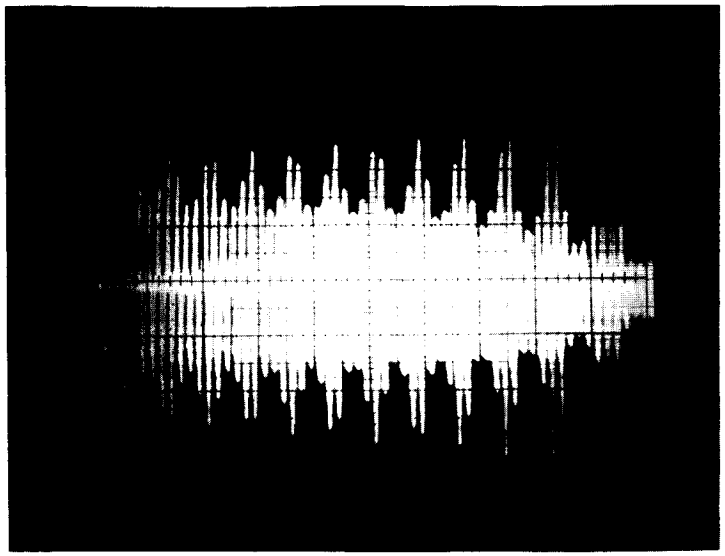

Fig. 2. Photograph Of The Open Loop Instability, Current Vs. Time. Time scale is 0.1 sec/cm.

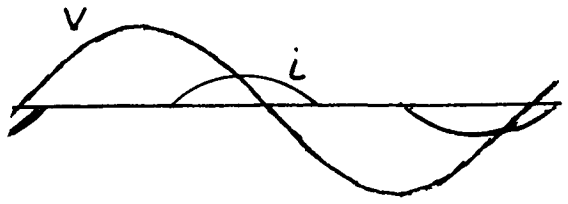

Fig. 3. Voltage And Current Vs. Time Waveforms for Single-Phase PFC.

effective voltage instead of a lower voltage as assumed above. The slip and the conventional power factor angle are now seen to increase and resist the original disturbance for this case, and the model is now consistent with the observed open loop stable behavior of the single-phase system. A stability test based on the improved model can be stated as follows. If the machine is acting as a generator at the moment of current shutoff, then the system is open loop stable. If the machine is acting as a motor at the moment of current shutoff, then the system has the potential to become open loop unstable.

The waveforms for the three-phase case with the motor neutral connected, are the same as the single-phase waveforms shown in Fig. 3, if the voltage waveform is redefined to be the line-to-neutral voltage and if the time axis is appropriately shifted for each phase [3]. With the neutral connected, a disturbance of a current shutoff affects the switching of the voltage applied to only the phase in which the disturbance occurs. Consequently, the stability argument is identical to the single-phase case, and the improved model is thus also consistent with the observed open loop stable behavior of the three-phase neutral-connected system.

When the neutral is not connected, Kirchoff's current law can be applied to the three inward-flowing stator currents i_A, i_B, and i_C to give

$$i_A + i_B + i_C = 0. \qquad \text{Eq. 1}$$

This equation clearly shows that a disturbance in the time of current shutoff in one phase also affects the current in at least one other phase. The problem can be stated in terms of voltage as follows. A disturbance in the time of current shutoff in one phase affects the switching of the voltages applied to all of the stator phases which are connected at the time. The model must be further refined to include this interaction. In other words, the effect of a disturbance in the time of current shutoff must be evaluated in terms of its total net impact on all three phases. The total net power supplied to the motor at any instant in time is given by

$$p(t) = (v_{AX})(i_A) + (v_{BX})(i_B) + (v_{CX})(i_C), \qquad \text{Eq. 2}$$

where A, B, and C are the terminals of the motor, X is an arbitrary reference point, and the currents are defined as before. For ideal SCR's/triacs, no distinction

is necessary between the motor terminals and the power supply lines in Eq. 2, because, with ideal switches, these points differ only when the current in a phase is zero. A distinction must, of course, be made between the power line neutral and the motor neutral; that is, if point X is selected to be "the" neutral, then the line neutral, or the motor neutral, must be consistently used in all three terms of Eq. 2.

A disturbance of the no-neutral system is easier to evaluate when the current humps are separate, because no more than two phases are connected at any one time during this case. This is the case defined as mode 2 by Lipo in Ref. 1. Typical separate-hump current waveforms, along with the corresponding line-to-neutral voltages are shown in Fig. 4. The quantity p(t) can be found by summing the products of current and voltages for each of three graphs in Fig. 4. This evaluates Eq. 2 with point X as the line neutral. If this is done for a point just before the shutoff of the first positive hump in Fig. 4, the A component of the power is positive, the B component is negative and larger than the A component, and the C component is zero. Since the B current hump is the return current for the A hump, the magnitudes of both currents are reduced identically by a left shift in the time of shutoff. It is thus shown that a early shutoff increases the net power to the motor, because the B term increases more than the A term decreases. Therefore, the shutoff of the first hump is open loop stable. Due to the symmetry of the waveforms, the calculation need not be repeated for the other shutoffs. For example, the second positive hump in A is the return for the first negative hump in C. The improved stability model is thus shown to be consistent with the observed behavior for the separate humps case.

The same calculation is more easily accomplished, if point X is taken to be point A. The waveforms are shown in Fig. 5. The A component of the power is now zero. The B component is negative, and the C component is zero. The disturbance of the A current enters the sum only through the B phase, and the same result as before is obtained directly from the B graph.

Additional insight can be obtained by repeating the calculation once more--this time with point X taken to be the motor neutral. The necessary voltage and current waveforms, along with the electrical torque, are shown in Fig. 6 for one phase. These waveforms are taken from Fig. 4B of Ref. 1. Only one phase needs to be shown, because the power is negative just before every shutoff. Since the symmetry means that this is true for all three phases, all non zero terms in Eq. 2 are shown to be negative just before shutoff. This again leads to the same result as before.

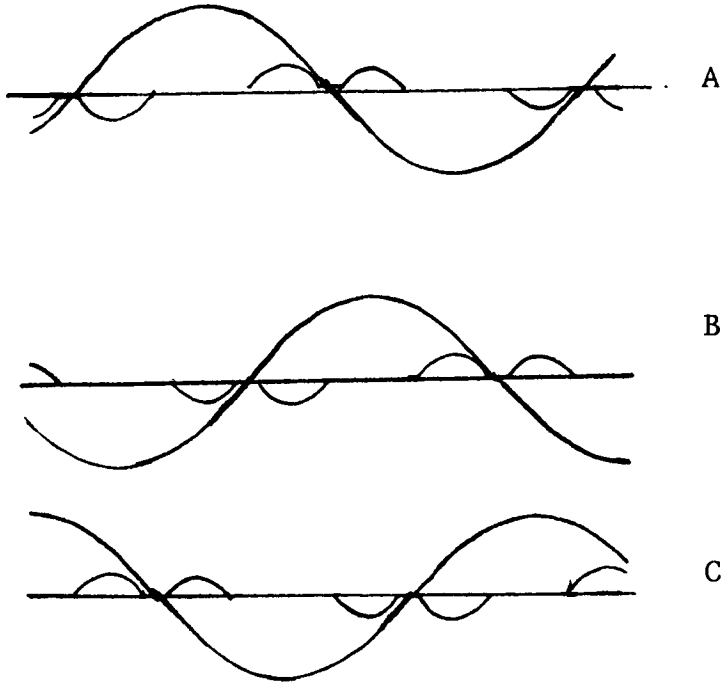

Fig. 4. Three-Phase Separate Current Humps Mode. Line-to-neutral voltages are also shown.

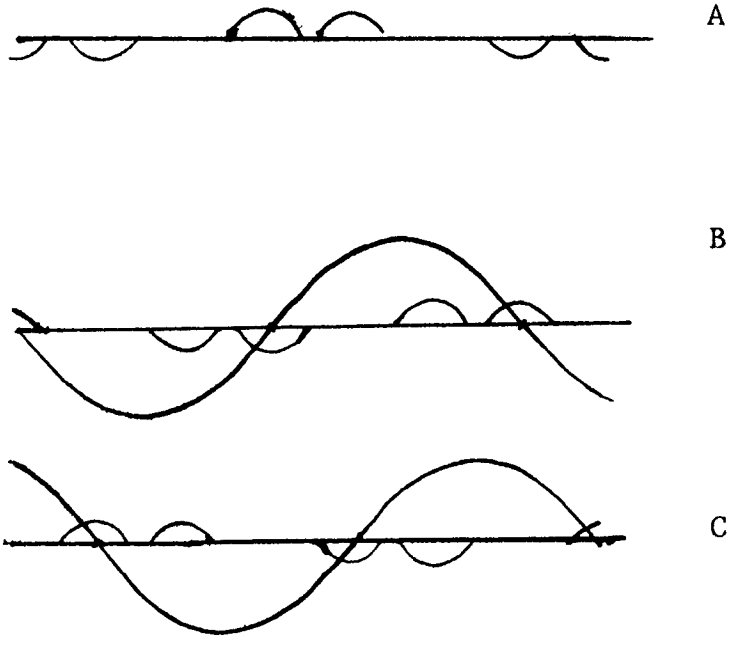

Fig. 5. Three-Phase Separate Current Humps Mode. Line-to-A voltages are also shown.

Observation of Fig. 6, shows that the torque is positive for both the motoring and generating portions of the cycle. This implies that the energy returned to the line during the generating portion of the cycle is energy from the inductors in the machine, not kinetic energy from the motor. Thus, the term "generating portion" is misleading, since it could be confused with the case where the rotor is driven above synchronous speed to produce actual generation.

It is interesting to note that, although a steady-state solution is obtained for the separate-humps, or mode 2, case in Ref. 1, the author of Ref. 1 in 1971 regarded this mode as useless, because it produced little torque. This mode is, of course, essential to achieving maximum power savings, at idle with a PFC.

A disturbance of the no-neutral system is harder to evaluate when the current humps overlap, because all three currents are affected by any shutoff disturbance. The difficulty arises, because a disturabnce in, say, i_A is split between i_B and i_C. The problem can be illustrated by the waveforms shown in Fig. 7. Near the positive A shutoff, i_B is positive and i_C is negative. Consequently, Eq. 1 can be rearranged for this case to obtain

$$|i_A| = |i_C| - |i_B|. \qquad \text{Eq. 3}$$

A left shift in the A shutoff reduces the magnitude of i_A, and therefore by Eq. 3, the magnitude of i_C must decrease or the magnitude of i_B must increase. Since opening one of the lines to the motor causes the potential of the motor neutral to jump away from ground potential, it is expected that both of these possibilities could occur. If both do occur, then the waveforms in Fig. 7 imply that the A and B terms in Eq. 2 have stabilizing effects, and that the C term has a destabilizing effect for ϕ less than 60°. Therefore, if the splitting factor favors the C term, in this manner, the system has the potential to be open loop unstable with the humps overlapped and ϕ less than 60°. Theis agrees reasonably well with the experimentally observed open loop unstable region.

Although definitive verification of the proposed open loop instability mechanism is not possible without better knowledge of the splitting factor, the argument for the proposed mechanism is persuasive, because this mechanism is the only apparent mode by which the motor

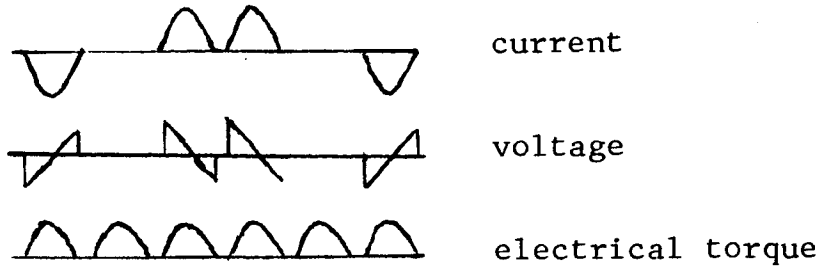

Fig. 6. Three-Phase Separate Humps Mode. Line-to-motor voltage is shown (After Ref. 1.)

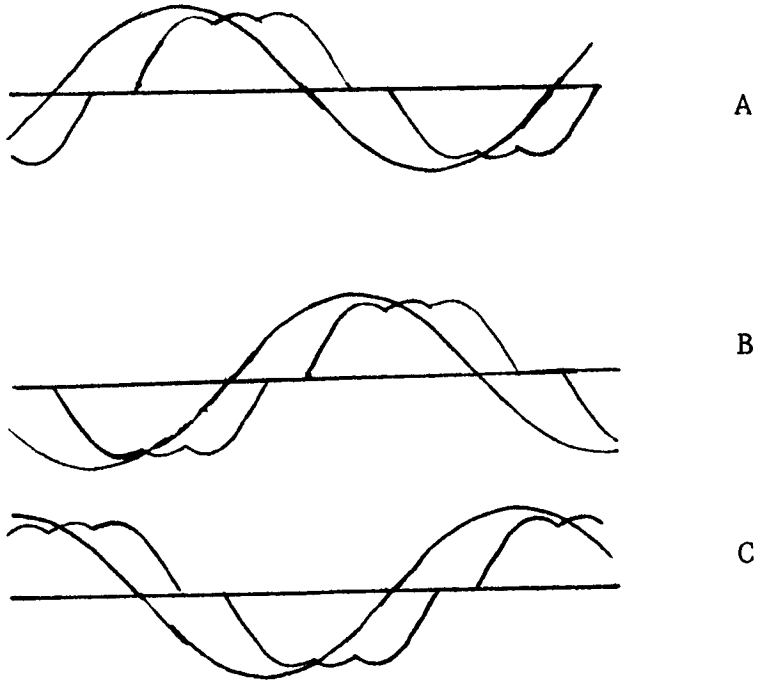

Fig. 7. Three-Phase Overlapped Humps Mode. Line-to-neutral voltages are shown.

can affect the switching of the voltage applied to itself, and because the shutoff time is experimentally observed to vary during the occurrence of the instability, and because the qualified predictions of the refined model agree with the observed stable and unstable cases.

The observed effects produced by adding inertia to the shaft can be readily explained by the model as follows. Sufficient inertia limits the change in slip that is initiated by a shutoff disturbance such that the shift in each successive shutoff is less than the one before and the disturbance is thereby damped out.

Perhaps the strongest experimental evidence to support the model, is that if the firing time is referenced to the previous current shutoff, the system becomes open loop stable. This is demonstrated by both the light-dimmer circuit shown in Fig. 8 and the current referenced modification of the Nola design shown in Fig. 9. This stable behavior is precisely predicted by the model as follows. A left shift of a current shutoff, for example, results in an earlier start for the next timing ramp, which in turn results in a left shift of the next current turn-on which nullifies the effect of the original shift.

As an additional test of the model, some observations were made on an antiparallel SCR-diode controller. No spontaneous initiation of the open loop instability is observed in this system [3]. The waveforms for this system are considerably different, and beyond the scope of this report, but the system is observed to operate in either of two modes. In one mode, no more than two phases are on at the same time and both phases are generators at the moment of shutoff. The waveforms of this mode are not the same as those of the separate-humps case of the SCR's/triac controller, but an almost identical argument can be used to show that this mode is stable. In the other mode, only one current shutoff occurs per cycle per phase. That is, the positive half of the current is not switched off at the zero crossing. Although the waveforms are again different, an almost identical argument can be used to show stability for this mode for ϕ greater than 60°, where ϕ is measured at the negative current shutoff. However, a potential for instability appears to exist for ϕ less than 60°. This is, of course, inconsistent with the observed behavior of this system. Either some other mechanism inhibits the instability or something is wrong with the model. The most obvious difference between the two systems is that the current shutoffs are spaced by 120° in the SCR-diode system, instead of the 60° of the SCR's/triac system. Perhaps the

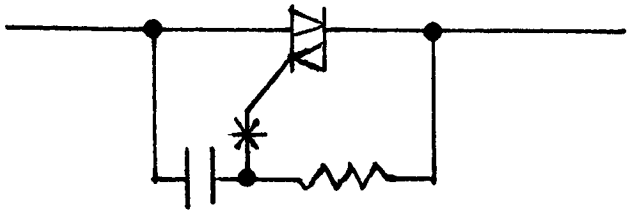

Fig. 8. Light-Dimmer Circuit for Controller. A unit is required for each phase.

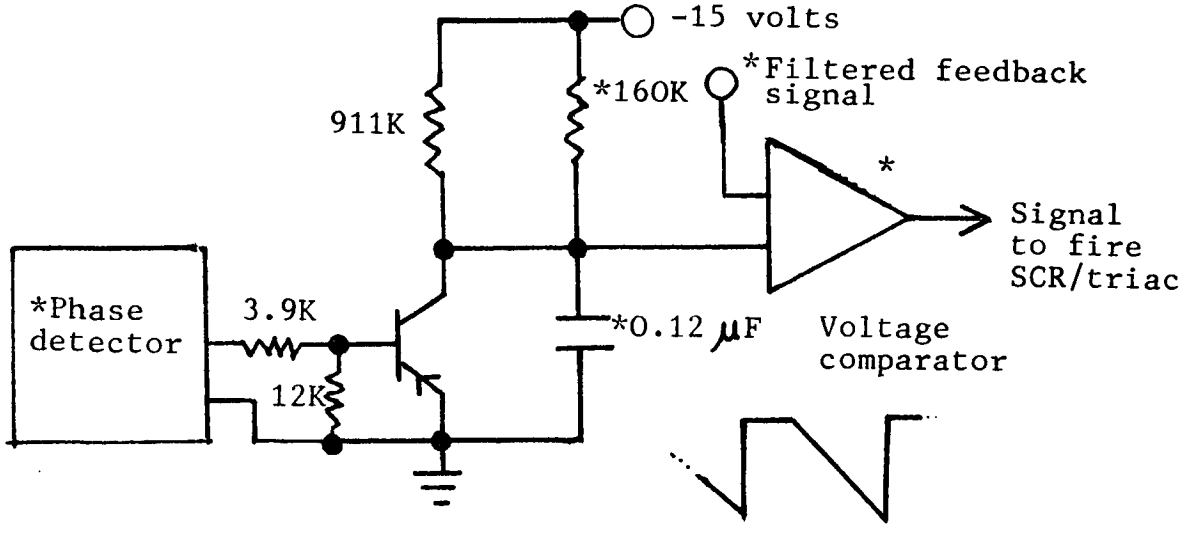

Fig. 9. Current-Referenced Modification of Nola Design. A unit is required to modify each phase. The modified timing-ramp waveform is also shown.

* Parts with * are part of Nola design.

additional time between current shutoffs allows the motor speed to restabilize sufficiently to limit the shift in the next shutoff to less than the original disturbance. This idea is supported by the experimental observation that the SCR-diode system with no added inertia reacts to a torque impulse the same way that the SCR's/triac system does with some inertia added to it; that is, they both exhibit similar damped oscillations in the expected unstable region [3].

The proposed open loop instability mechanism imposes two constraints on a closed loop system: (1) the times of current shutoff, or a parameter which quickly reacts to them must be sensed, and (2) the response of the feedback path must be rapid enough to correct the next gate firing. These design rules are particularly important for a PFC, since many important PFC applications involve operating conditions that could evoke the open loop instability mechanism. Note that the design rules imply that it is best to sense both polarities of all three phases and to independently time the gate firings of each phase. Note also that an optical tach with only one "blip" on the shaft is predicted to provide too slow a sample for the feedback signal.

As described in the introduction, the Nola design clearly meets the first design constraint. The Nola design is shown to meet the second constraint by the graph shown in Fig. 10. The graph is a computer plot of the response of the feedback filter from the Nola design when the input is a 33.3% duty cycle square wave interrupted by a single period with a 16.7% duty cycle. This input simulates a 10^{o} left shift in an otherwise steady-state power factor of 20^{o}. The output clearly responds to the disturbance within the 60^{o} "subcycle" in time to correct the next gate firing, if the slope of the timing ramps is correct. This is verified in the next section.

BOUNDS ON THE 50- AND 200-HZ POLES

Comparison of Fig. 10 with Fig. 11, which is the same as Fig. 10, but without the 200-Hz pole, indicates that the 200-Hz pole acts to smooth (integrate) the points off the ripple. Closer comparison indicates that the 200-Hz pole also reverses the curvature of the "straight" portions of the waveform. The significance of this can be illustrated if the 200-Hz pole is removed from the actual system by disconnecting the 0.056 μF capacitor. An operating region can then be found where a ripple slope matches to the slope of a

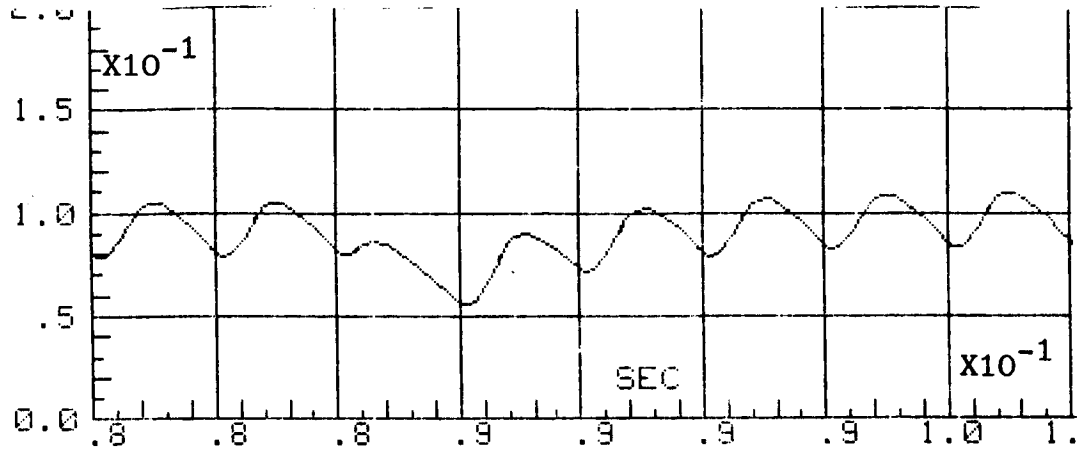

Fig. 10. Normalized Plot Of The Response Of The Feedback Signal Filter Of The Nola Design To A 10^{o} Left Shift In An Otherwise Constant 20^{o} Conventional Power Factor Angle. To obtain actual voltage, multiply the plot by -11.7 volts. The large horiaontal divisions are 60^{o}.

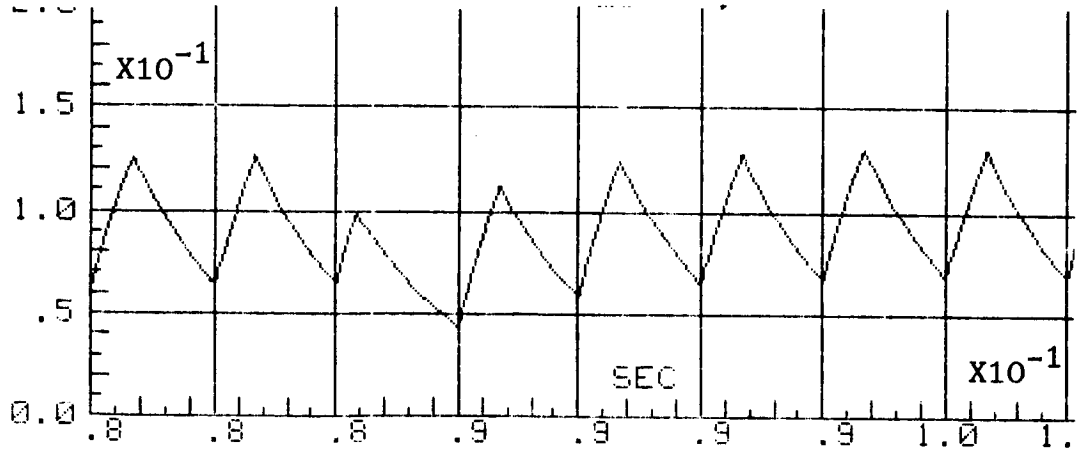

Fig. 11. Same plot as Fig. 10, but with the 200-Hz pole omitted.

timing ramp and the firing point is observed to jump erratically from end to end of the ripple. A photograph illustrating this is shown in Fig. 12.

Since the downward portion of the ripple cannot match to an upward timing ramp, the function of the 200-Hz pole is to shape the upward (on the normalized plots) portion, which lasts some 50^{o} or less for normal "PFC adjust" settings. This response is set in the Nola design by the 0.056μF capacitor and the 12K ohm thevenin resistance which charges it. At the end of 50^{o}, the response of this pole is down to 6%, which is large enough to shape the ripple, yet small enough not to slow the overall response of the filter unnecessarily. That is, the 200-Hz pole is just low enough to shape the ripple without unduly restricting the bandwidth of the filter. The "200-Hz" pole, incidently, is at 189 Hz with the diodes off and at 237 Hz with the diodes on.

The 50-Hz pole needs to be high to provide the fast response required to control the open loop instability, but it cannot be raised too high or the 200-Hz pole cannot shape the ripple. For the necessary curvature, the following inequality must be satisfied:

$$(2\pi f_2)^2 \exp(-2\pi f_2 t) \leq (2\pi f_1)^2 \exp(-2\pi f_1 t), \quad \text{Eq. 4}$$

where f_1 is the 50-Hz pole, f_2 is the 200-Hz pole, and t is the longest expected time for the normalized upward (actual downward) portion of the ripple. For f_2 set by 12K ohms and 0.056μF as before, and f_1 = 50 Hz, the curvature will be correct for up to 57^{o}, which means that the 50-Hz pole is properly located to obtain the fastest response while maintaining the curvature.

Observation of Fig. 10 shows that the slope of the ripple is the response of the filter to a shutoff disturbance. Since the response of the 200-Hz pole is virtually over after five time constants, and since the ripple slope is approximately constant, the slope is approximated by:

$$\text{ripple slope} = 2\pi f_1 G_a V_h \exp(-5f_1/f_2), \quad \text{Eq. 5}$$

where G_a is the AC gain of the "flat" portion of the Bode plot between 0.7 and 50 Hz, and V_h is the height of the square wave whose duty cycle represents the power factor angle. For the plot in Fig. 10, V_h is normalized to +1 volt, and the DC gain is normalized to +1. Therefore $G_a V_h$, for the normalized plot, is about 0.22, and Eq. 5 predicts a normalized slope of 20. The slope of Fig. 10 is 17; therefore, Eq. 5 is a reasonable approximation as long as f_1 and f_2 are related properly to control the slope as described above.

The graph in Fig. 10 shows that a 10^{o} left shift

in the time of shutoff results in a 0.025 normalized voltage drop. This corresponds to an actual drop of 0.297 volts. (The DC gain times V_h is 11.7.) The slope of the timing ramp is 781 volts/sec, resulting in a correction of the next firing angle by 8.2^{o}. This means that the slope of the filter is properly set.

FUNCTION OF 6^{o} DELAY

Observation of Fig. 4, which shows a typical idle current waveform, reveals that the second hump starts after the zero crossing of the line-to-neutral voltage. The second hump in the A phase starts when the first hump is triggered in the C phase, but the A phase SCR's/triac must have a gate signal at this time to allow it to switch on and provide the return path for the C phase. This requires the timing ramps to be delayed 6^{o} past the line-to-neutral zero crossings. The necessary delay is provided in the Nola design by the 0.039 μF capacitors in the voltage dividers that sample the line-to-neutral voltage.

DISCUSSION OF POSSIBLE NOISE REDUCTION TECHNIQUES

The photograph in Fig. 13 shows a typical waveform for the noise voltage observed between the derived neutral and the line neutral. As mentioned in the introduction, this noise is not observed to produce any significant effect on the operation of the system. This noise could be reduced, if desired for a particular application, by lowering

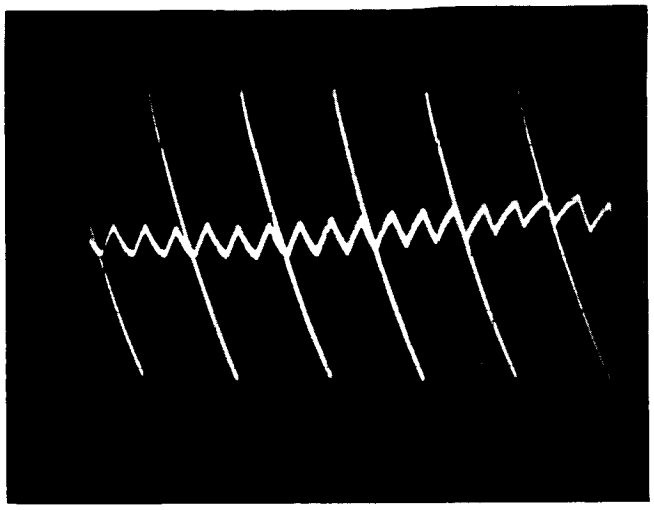

Fig. 12. Matching Of Ripple Slope To The Slope Of The Timing Ramp. Note that the voltage is inverted from the normalized plots. Ground reference is at the top of ramps. The firing point changes on the fourth ramp shown. Vertical scale is 1 volt/div. and the ramps are 60^{o} wide.

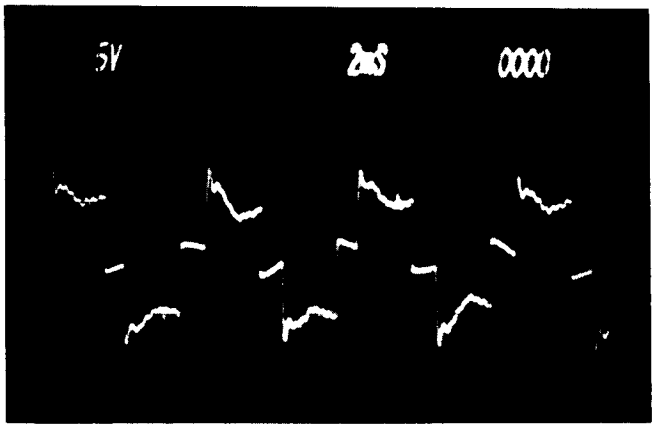

Fig. 13. Typical Noise Observed On The Derived Neutral.

the size of the resistors in the line-to-neutral voltage dividers. The 0.039 μF capacitors should be raised as needed to maintain the 6° shift. Alternatively, the derived neutral could be grounded to the line neutral to eliminate the noise, if a suitable line neutral were available (It should be mentioned that the open loop instability is observed to occur even with the derived neutral so grounded.) Also, it is significant to note that the noise on a not-entirely-firm derived neutral might serve a useful function. This is based on the observation that when some faults are deliberately introduced into the circuit, the resulting imbalance of the derived neutral tends to limit the consequences of those faults.

A small amount of noise from the gatepost oscillator can be detected on the inputs of the voltage comparators which control the gate firings. The noise is barely visible on the scope, and it produces no observable effects, but it can be reduced by placing 0.01μF capacitors from these inputs to ground. A significantly larger capacitance should not be used, because it would undesriably alter the feedback filtering. The inputs from the timing ramps of course, need not and should not be filtered.

OPTICAL TRIGGERING OPTION

Experimental observations from two optically coupled trigger circuits are reported in this section. The first circuit is shown in Fig. 14 and the second circuit, which is not shown, differs from Fig. 14 only on the gate side of the coupler, where a DC gate signal is employed. Observations of both circuits demonstrate that the open loop instability occurs without the gatepost oscillator. For example, the photograph in Fig. 1 was taken with DC optical triggering and with the derived neutral grounded.

Switching circuitry to provide separate triggering for each polarity is shown in Fig. 15, in case this is desired for a particular application. However, this circuit is observed to not function properly in the separate-humps mode. The malfunction is probably due to confusion of the power-factor-angle sensor when the off SCR is not triggered between the humps. If so, supplying a signal to "hold on" the angle sensor during the time of the gate trigger should correct the problem. It should be mentioned that optically coupled SCR's--not triacs--should be used for SCR triggering, since triacs, in response to a line transient, might "turn on" the gate of the off SCR without gating the on SCR and this might exceed the reverse gate breakdown voltage of the main SCR and destroy the coupler and/or the main SCR.

CALCULATION OF POWER FACTOR REDUCTION FOR A MIXED LOAD

A loaded 240-volt motor was observed to draw 2700 watts and 8.7 amps. This is a volt-amp draw of 3616.5 VA, which implies a power factor of 2700/3616.5 = 0.75. The same motor, at idle, drew 315 watts and 5.65 amps. This is a volt-amp demand of 2348.6 VA, which implies a power factor of 0.13. Forming the phasor sum of the currents from both motors shows that the power factor of the combined load would be 0.54.

The same motor, with a PFC, was observed to draw 2700 watts and 8.8 amps when loaded. This is a volt-amp draw of 3658, which implies a power factor of 0.74. The same motor with the PFC was observed to draw 70 watts and only 1.48 amps at idle. This is a volt-amp draw of 615 VA, which implies a power factor of 0.11. This is essentially the same power factor as without the PFC, but yet the reactive current was greatly reduced. The apparent paradox is resolved by calculating the power factor for the combined load with the PFC's. Due to the nonsinusoidal current waveform, the currents were added point by point as shown in Fig. 16. The rms value of the combined currents is 9.7 amps, which implies a volt-amp draw of 4032 VA and a power factor of 0.69--a marked improvement from the 0.54 without the PFC's. The reason that the PFC does not appear to significantly improve the power factor of a single motor, is merely because the PFC reduces the real power in addition to reducing the reactive power. However, the calculation based on Fig. 16, demonstrates that for actual plant conditions the power factor is reduced. It is significant to note that the power factor of a plant would need little power factor correction if some motors were not idling or partly loaded at the time the power factor is measured. This is pointed out by Mr. Nola in the rebuttal published with Ref. 5.

Fig. 14. Optical Triggering Circuit. Three units are required.

Parts with * are part of Nola design.

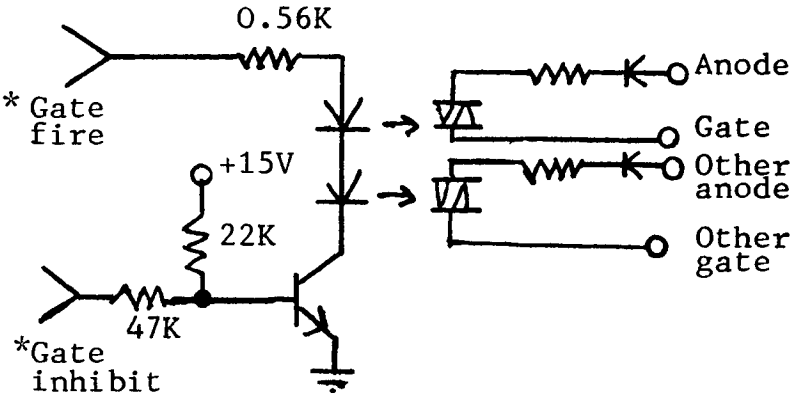

Fig. 15. Alternate Polarity Trigger Circuit. See text.

Outputs of couplers are same as Fig. 14.

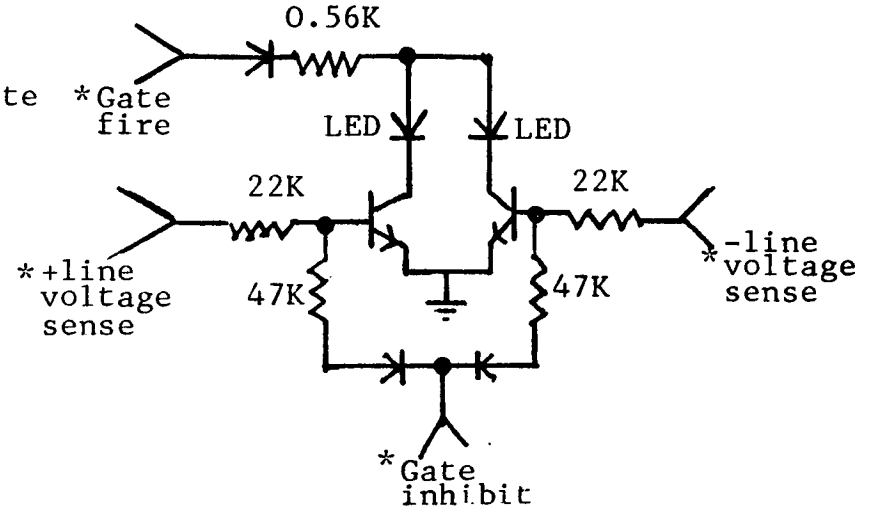

Fig. 16.

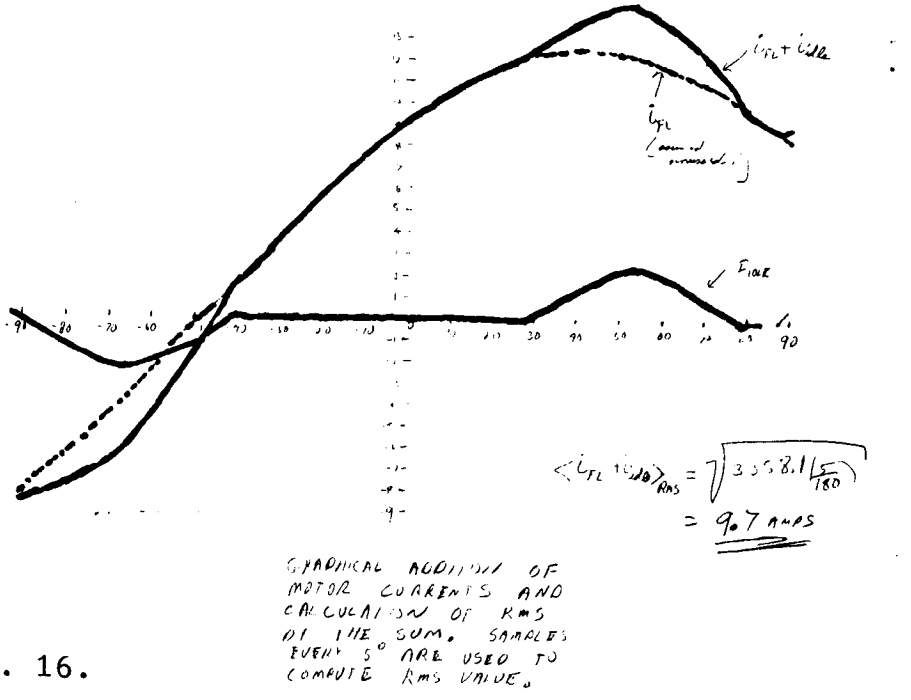

AREAS FOR FUTURE WORK

The most obvious area for future work is determination of the splitting factor for a disturbance in the time of switching from three lines to two lines. Since the disturbance seems to imply a nonsymmetric shift of the currents, three current probes with a storage scope would constitute a useful means to check the observed disturbance for nonsymmetry and aid further understanding of the phenomenon. Additional observation of the SCR-diode system, perhaps with a specially-constructed low inertia motor, might resolve the question of its stability. A separate-polarity triggering system--probably best implemented with optical coupling--is expected to simplify modification of the system to accept a remote control signal. Investigation of the region where only one line is switched on at a time should also benefit this application. This operating region cannot and need not, occur in the Nola design, but it might occur in a version modified to accept remote control. Contrary to some opinion, current does flow in this region--through the snubber circuits--and this is significant because it might induce violent misfiring, just before the intended turnon of the motor.

CONCLUSIONS AND RECOMMENDATIONS

The Nola design meets the design constraints imposed by the open loop instability mechanism modeled in this report. The empirically determined parameters are optimally set between the limits demonstrated in this report. Equations 4 and 5 might be used to shift the 50- and 200-Hz poles somewhat and maintain a suitable slope and curvature, but this is not needed for any reason considered in this study, and it might adversely affect the good servo loop response that the system was experimentally observed to exhibit. Consequently, it is recommended that the parameters not be changed. Finally, it is strongly recommended that the splitting factor be investigated--not only because it is an interesting academic problem--but also because the open loop instability phenomenon is basic to any SCR's/triac motor controller, with no neutral.

REFERENCES

1. Lipo, T.A., "The Analysis of Induction Motors With Voltage Control by Symmetrically Triggered Thrysistors," IEEE Transactions on Power Apparatus and Systems, Vol. PAS-90, No. 2, 1971.

2. Toms, J.W., "Applying Solid State Energy Saver Starters," IEEE 1982 Annual Textile Industry Technical Conference, IEEE Catalog No. 82-CH1777-2, May 1982.

3. Nola, F.J., personal communication.

4. Rowan, T.M. and Lipo, T.A., "A Quantitative Analysis of Motor Performance Improvement by SCR Voltage Control," to be published.

5. Posma,B., "A Sober Look at Power Factor Controllers and Energy Savers," Power Conversion International, to be published Fall 1982.
(See also the rebuttal paper by F. J. Nola in the same issue.)